Estimation of Permanent Magnet Synchronous Motor Parameters using a Linear Unknown Input Interval Observer

Elinirina I. Robinson*
KBR, Inc., NASA Ames Research Center, Moffett Field, CA 94035, USA

Wendy A. Okolo†
NASA Ames Research Center, Moffett Field, CA 94035, USA

This paper develops and evaluate a technique to estimate the speed and unknown load torque of a permanent magnet synchronous motor (PMSM). An interval unknown input observer (UIO) for linear time-invariant (LTI) systems is designed and utilized to estimate the PMSM parameters. Interval UIOs are advantageous as they allow for the estimation of both states and unknown inputs, while accounting for varying uncertainty sources, such as model and measurement uncertainties inherent in dynamic systems and processes. First, the nonlinear PMSM model is linearized to transform it to a suitable form for application of the linear interval UIO. Then, the interval UIO is applied to jointly estimate the motor speed and the unknown load torque disturbance. Assuming that the measurement noise and disturbances are bounded, lower and upper bounds are first computed for the unmeasured state (motor speed) and then for the unknown input (load torque). The proposed approach and its limitations are demonstrated for the nonlinear PMSM model derived from its equivalent electrical circuit.

I. Introduction

Emerging Urban Air Mobility (UAM) operations are expected to revolutionize transportation in moderate to densely populated urban areas by providing an air transportation system that can safely, efficiently, and autonomously move people and cargo 1, 2. These operations, in rural and urban metropolitan regions, will vary from aerial medical services for patients and/or medical supplies, large package delivery, and personal taxi services using a variety of autonomous aircraft types.

With this widespread interest stemming from the vast potential of UAM vehicles and operations, electric propulsion powered aircraft are under investigation as their vertical takeoff and landing capabilities can enable UAM operations in constrained spaces. Furthermore, electric propulsion systems provide the added benefits of reduced noise and pollution levels associated with the usage of jet fuel required for conventional fixed-wing aircraft 3. On the other hand, the propulsion systems of electric aircraft have significantly reduced energy capabilities in comparison to their jet fuel counterparts, thus limiting their range and endurance. This will pose a unique set of safety challenges that necessitate accurate characterization of UAM propulsion systems to enable prediction and mitigation of hazards that could arise from their use.

With the goal of diagnosing, predicting, and mitigating risks to safe UAM operations by first developing accurate models that represent critical UAM components, this paper investigates a technique to estimate the parameters of the permanent magnet synchronous motor (PMSM), an electric motor with significant potential for use in UAM vehicle design. The PMSM is gaining interest in the UAM industry because it has high efficiency and high power density while remaining a relatively small motor with reduced noise levels 4, 5.

The implementation of a diagnostic technique that can enable fault detection, identification, and isolation, can be achieved using the speed and load torque of the PMSM. However, mechanical sensors that can provide these necessary parameters may not always be included in the design by the original equipment manufacturer (OEM). Thus, estimating the speed and load torque of the PMSM reduces reliance on these sensors and enables the overall diagnostics of the electric power train that depends on electro-mechanical components including the motor and battery.

Although there are varying techniques of motor speed and load torque estimation, this work utilizes an observer-based approach that can handle parameter uncertainties in the motor model to improve accuracy and provide robustness.

*Research Engineer, Intelligent Systems Division.
†Aerospace Research Engineer, Intelligent Systems Division, MS 269-1, AIAA Member

Specifically, the interval Unknown Input Observer (UIO) technique for linear time-invariant (LTI) systems is chosen for its capability to estimate both state and unknown inputs in the presence of disturbances that cannot be measured.

This paper is organized as follows. First we give an overview of the PMSM in Section II along with its nonlinear and linearized equations. This is followed by a description of the interval UIO design in Section III. Then, we describe the application of the interval UIO to the estimation of the PMSM speed and load torque disturbance in IV, after which we give a discussion and analysis of results. Finally, a conclusion and guide to future work is presented in Section V.

II. Permanent Magnet Synchronous Motor Model

In this section, the nonlinear equations of the PMSM model are described in two reference frames - the three-phase abc frame and a simplified, two-phase synchronous reference frame called the $d-q$ frame. This is followed by the linear equations utilized in the UIO design.

A. Nonlinear PMSM motor equations

The PMSM model, derived from its equivalent circuit model, has been widely studied and used in the literature [6]. It has been established under the following assumptions:

- Stator windings are symmetrical, three-phase.
- Rotors have non-salient poles with surface-mounted magnets.
- Saturation and hysteresis losses in the magnetic circuit, as well as eddy currents in the armature are neglected.
- The induced electromagnetic force (EMF) is sinusoidal.

1. Electrical equation

Under the defined assumptions, the voltage equation of the PMSM in the abc reference frame is given by:

$$\mathbf{v}_{abc} = \begin{bmatrix} R_s & 0 & 0 \\ 0 & R_s & 0 \\ 0 & 0 & R_s \end{bmatrix} \mathbf{i}_{abc} + \frac{d\boldsymbol{\lambda}_{abc}}{dt} \tag{1}$$

where $\mathbf{v}_{abc}$, $\mathbf{i}_{abc}$ and $\boldsymbol{\lambda}_{abc}$ are the voltage, current and flux linkage vectors of the three phases, respectively, and R_s is the phase resistance.

The flux linkage vector is expressed as

$$\boldsymbol{\lambda}_{abc} = \begin{bmatrix} L_s & M & M \\ M & L_s & M \\ M & M & L_s \end{bmatrix} \mathbf{i}_{abc} + \lambda_M \begin{bmatrix} \cos(\theta_r) \\ \cos(\theta_r - \frac{2\pi}{3}) \\ \cos(\theta_r + \frac{2\pi}{3}) \end{bmatrix} \tag{2}$$

where L_s is the phase self inductance, M is the mutual inductance, λ_M is the peak strength of the flux linkage due to the magnets, and θ_r is the electrical position of the rotor. This electrical position is defined by the angle between the rotor flux and the stator phase a. It is a function of the rotor mechanical angle θ_m, and can be expressed as $\theta_r = n_p\theta_m$, where n_p is the number of poles.

After substituting Eq. 2 into Eq. 1, the electrical equation of the PMSM in the abc frame becomes

$$\mathbf{v}_{abc} = \begin{bmatrix} R_s & 0 & 0 \\ 0 & R_s & 0 \\ 0 & 0 & R_s \end{bmatrix} \mathbf{i}_{abc} + \begin{bmatrix} L_s & M & M \\ M & L_s & M \\ M & M & L_s \end{bmatrix} \frac{d\mathbf{i}_{abc}}{dt} - \lambda_M \omega_r \begin{bmatrix} \sin(\theta_r) \\ \sin(\theta_r - \frac{2\pi}{3}) \\ \sin(\theta_r + \frac{2\pi}{3}) \end{bmatrix} \tag{3}$$

where ω_r is the electrical angular velocity of the PMSM ($\omega_r = n_p\omega_m$).

2. Mechanical equation

A complete description of the PMSM behavior that depends on the rotor position and angular speed, requires that the mechanical equation of the PMSM, derived from Newton's second law, is included in the model:

$$\frac{d\omega_r}{dt} = \frac{n_p}{J}(T_e - T_l - B_f\omega_r) \tag{4}$$

where n_p is the number of pole pairs, J is the inertia of the rotor, B_f is the viscous friction coefficient, T_e is the electromagnetic torque, and T_l is the load torque of the motor.

The electromagnetic torque T_e is given by

$$T_e = -n_p \mathbf{i}_{abc}^{\top} \lambda_M \omega_r \begin{bmatrix} \sin(\theta_r) \\ \sin(\theta_r - \frac{2\pi}{3}) \\ \sin(\theta_r + \frac{2\pi}{3}) \end{bmatrix} \tag{5}$$

3. PMSM equations in $d-q$ frame

The previous equations describing the PMSM behavior in the abc stationary frame attached to the stator depend on the rotor position θ_r. To remove this dependency and thus simplify the equations, the Park transform is used to obtain a set of equations in the $d-q$ rotating frame attached to the rotor, where the voltage, current and flux vectors have two DC components instead of three AC components [7].

The Park transform to convert from the three-axis stationary frame abc to the rotating frame $d-q$ and inversely, can be written as

$$\mathbf{f}_{dq} = P_{abc \to dq} \mathbf{f}_{abc}$$
$$\mathbf{f}_{abc} = P_{dq \to abc} \mathbf{f}_{dq}$$

where $\mathbf{f}_{dq}$ and $\mathbf{f}_{abc}$ describe the PMSM equations in the $d-q$ and abc frames, respectively. The Park transform matrices are given by

$$P_{abc \to dq} = \begin{bmatrix} \cos(\theta_e) & \sin(\theta_e) \\ -\sin(\theta_e) & \cos(\theta_e) \end{bmatrix} \quad \text{and} \quad P_{dq \to abc} = \begin{bmatrix} \cos(\theta_e) & -\sin(\theta_e) \\ \sin(\theta_e) & \cos(\theta_e) \end{bmatrix} \tag{6}$$

After applying the Park transform to the variables in the abc frame, the following equations of the PMSM in the $d-q$ frame are obtained:

$$v_d = R_s i_d - L_q i_q \omega_r + L_d \frac{di_d}{dt} \tag{7}$$

$$v_q = L_d \omega_r i_d + R_s i_q + L_q \frac{di_q}{dt} + \lambda_M \omega_r \tag{8}$$

$$T_e = \frac{3}{2} n_p \lambda_M i_q \tag{9}$$

$$\frac{d\omega_r}{dt} = \frac{n_p}{J}(T_e - T_l - B_f \omega_r) \tag{10}$$

where v_d,v_q and i_d, i_q are the voltage and current components, respectively, in the $d-q$ axis, and L_d,L_q are the direct and quadrature inductances, respectively. Note that for a surface-mounted PMSM, the synchronous inductances, L_d and L_q, are equal since the permanent magnets are mounted on the surface, causing equal reluctance in every position. Thus, $L_d = L_q = L_s$ [8], where L_s is simply the synchronous inductance of the surface-mounted PMSM.

By denoting the state vector by $\mathbf{x} = [i_d \;\; i_q \;\; \omega_r]^T$, the input vector by $\mathbf{u} = [v_d \;\; v_q]^T$, and the unknown load torque by $d = T_L$, the state-space representation of the non-linear PMSM in the $d-q$ frame is

$$\dot{\mathbf{x}} = f(\mathbf{x}, \mathbf{u}) + Dd \tag{11}$$

with

$$f(\mathbf{x}, \mathbf{u}) = \begin{bmatrix} -\frac{R_s}{L_s} i_d + i_q \omega_r + \frac{1}{L_s} v_d \\ -\omega_r i_d - \frac{R_s}{L_s} i_q - \frac{\lambda_M}{L_s} \omega_r + \frac{1}{L_s} v_q \\ \frac{3n_p^2}{2J} \lambda_M i_q - \frac{B_f}{J} \omega_r \end{bmatrix} \quad \text{and} \quad D = \begin{bmatrix} 0 \\ 0 \\ \frac{n_p}{J} \end{bmatrix} \tag{12}$$

B. Linearization of the PMSM model

To apply a linear interval UIO to estimate the PMSM speed and unknown load torque, the Jacobian linearization of the non-linear PMSM model in Eq. (11) around an operating point $\mathbf{x_0} = [i_{d_0} \;\; i_{q_0} \;\; \omega_{r_0}]$ is used:

$$\Delta\dot{\mathbf{x}} = \underbrace{\begin{bmatrix} -\frac{R_s}{L_s} & \omega_{r_0} & i_{q_0} \\ -\omega_{r_0} & -\frac{R_s}{L_s} & -\frac{\lambda_M}{L_s} - i_{d_0} \\ 0 & \frac{3n_p^2}{2J}\lambda_M & -\frac{B_f}{J} \end{bmatrix}}_{A_J} \Delta\mathbf{x} + \underbrace{\begin{bmatrix} \frac{1}{L_s} & 0 \\ 0 & \frac{1}{L_s} \\ 0 & 0 \end{bmatrix}}_{B_J} \Delta\mathbf{u} - \begin{bmatrix} 0 \\ 0 \\ \frac{n_p}{J} \end{bmatrix} d \tag{13}$$

where $\Delta\mathbf{x}$ and $\Delta\mathbf{u}$ are deviation variables from the operating/linearization point, and $A_J = \frac{\partial f}{\partial \mathbf{x}}\Big|_{\substack{\mathbf{x}=\mathbf{x_0} \\ \mathbf{u}=\mathbf{u_0}}}$ and $B_J = \frac{\partial f}{\partial \mathbf{u}}\Big|_{\substack{\mathbf{x}=\mathbf{x_0} \\ \mathbf{u}=\mathbf{u_0}}}$ are the Jacobian matrices derived from $f(\mathbf{x}, \mathbf{u})$ and evaluated at the operating/linearization point.

The resulting linearized model in Eq. (13), can now be used to estimate the bounds of the state and unknown inputs using the linear interval UIO described in the next section. In this case, $\mathbf{x}$ is the state vector and d is the unknown input associated with the load torque disturbance.

III. Unknown Input Interval Observer Design

A. Problem Statement and Methodology

The complete design procedure of the interval UIO is described in Ref. [9], and this interval UIO design has been successfully applied to the prognosis of a suspension system degradation in Ref.[10]. The unknown input interval observer designed in this paper is based on the UIO proposed in Ref. [11], whose methodology is extended to systems with bounded disturbances and noise.

In the context of an LTI system for which a linear UIO can be designed, consider the following LTI discrete-time system:

$$\begin{cases} x(k+1) &= Ax(k) + Bu(k) + Dd(k) + \omega(k) \\ y(k) &= Cx(k) + \delta(k) \end{cases} \tag{14}$$

where $x \in \mathbb{R}^n$, $u \in \mathbb{R}^m$ and $y \in \mathbb{R}^p$ are the state, the input and the measurement vectors, respectively and $d \in \mathbb{R}^q$ is the unknown input vector, which does not affect the outputs. A, B, C and D are the linear time invariant matrices of appropriate dimensions. Finally, $\omega \in \mathbb{R}^n$ and $\delta \in \mathbb{R}^p$ are the state and measurement noises which are assumed to be bounded with a priori known bounds $\overline{\omega}$ and $\overline{\delta}$, respectively. Thus, $|\omega| \leq \overline{\omega}$ and $|\delta| \leq \overline{\delta}$ where $\overline{\omega} \in \mathbb{R}^n$ and $\overline{\delta} \in \mathbb{R}^p$ are constant component-wise positive vectors and $|\cdot|$ is the component-wise absolute value for vectors. Moreover, it is assumed that $n \geq q$ and $p \geq q$.

Following a change of coordinates, the state of the system can be divided into two subsystems, one dependent on the unknown input and the other having no dependence on the unknown input. This allows the design of an interval observer in the new coordinate basis to estimate the upper and lower bounds of the state. Then, by returning into the initial coordinates, the upper and lower bounds of the unknown input can be computed. First of all, the following assumptions are required:

Assumption 1 *C is a full row rank matrix and D is a full column rank matrix.*

Under Assumption 1, there exists an orthogonal matrix $H \in \mathbb{R}^{n\times n}$ and matrices $R_0 \in \mathbb{R}^{q\times q}$ and $K \in \mathbb{R}^{q\times q}$ such that:

$$D = H \begin{bmatrix} R_0 \\ 0 \end{bmatrix} K^T \tag{15}$$

This leads to the transformation of system in Eq. (14) into an equivalent one:

$$\begin{cases} z(k+1) &= \tilde{A}z(k) + \tilde{B}u(k) + \begin{bmatrix} R_0 \\ 0 \end{bmatrix} \tilde{d}(k) + \tilde{\omega}(k) \\ y(k) &= \tilde{C}z(k) + \delta(k) \end{cases} \tag{16}$$

where:

$$H = \begin{bmatrix} H_{11} & H_{12} \\ H_{21} & H_{22} \end{bmatrix}, \quad \tilde{A} = H^T A H = \begin{bmatrix} \tilde{A}_{11} & \tilde{A}_{12} \\ \tilde{A}_{21} & \tilde{A}_{22} \end{bmatrix}$$

$$\tilde{B} = H^T B = \begin{bmatrix} \tilde{B}_1 \\ \tilde{B}_2 \end{bmatrix}, \quad \tilde{C} = CH = \begin{bmatrix} \tilde{C}_1 & \tilde{C}_2 \end{bmatrix}$$

$$z(k) = H^T x(k) = \begin{bmatrix} z_1(k) \\ z_2(k) \end{bmatrix}, \quad \tilde{d}(k) = K^T d(k)$$

$$\tilde{\omega}(k) = H^T \omega = \begin{bmatrix} \tilde{\omega}_1(k) \\ \tilde{\omega}_2(k) \end{bmatrix}$$

H^T is supposed to be bounded, therefore $|\tilde{\omega}| \leq \overline{\tilde{\omega}}$ where $\overline{\tilde{\omega}}$ is a constant positive vector. The system in Eq. (16) is decomposed into an unknown input dependent subsystem and an unknown input-free subsystem described by:

$$\begin{cases} z_1(k+1) & = \tilde{A}_{11} z_1(k) + \tilde{A}_{12} z_2(k) + \tilde{B}_1 u(k) + R_0 \tilde{d}(k) + \tilde{\omega}_1(k) \\ z_2(k+1) & = \tilde{A}_{21} z_1(k) + \tilde{A}_{22} z_2(k) + \tilde{B}_2 u(k) + \tilde{\omega}_2(k) \\ y(k) & = \tilde{C}_1 z_1(k) + \tilde{C}_2 z_2(k) + \delta(k) \end{cases} \tag{17}$$

where $\tilde{C}_1 \in \mathbb{R}^{p \times q}$ and $\tilde{C}_2 \in \mathbb{R}^{p \times (n-q)}$.

$\tilde{C}_1$ is supposed to be a full column rank matrix [12] and can be decomposed as:

$$\tilde{C}_1 = H_1 \begin{bmatrix} R_1 \\ 0 \end{bmatrix} K_1^T \tag{18}$$

where $H_1 = \begin{bmatrix} H_{011} & H_{012} \end{bmatrix}$ ($H_{011} \in \mathbb{R}^{p \times q}$ and $H_{012} \in \mathbb{R}^{p \times (p-q)}$) and $\tilde{y}(k) = H_1^T y(k)$; the measurements equation can be decomposed as

$$\begin{cases} \tilde{y}_1(k) & = R_1 K_1^T z_1(k) + H_{011}^T \tilde{C}_2 z_2(k) + H_{011}^T \delta(k) \\ \tilde{y}_2(k) & = H_{012}^T \tilde{C}_2 z_2(k) + H_{012}^T \delta(k) = C_2 z_2(k) + H_{012}^T \delta(k) \end{cases} \tag{19}$$

As $\tilde{y}_1(k) = G_s^T \tilde{y}(k)$ with $G_s^T = \begin{bmatrix} I_q & O_{q \times (p-q)} \end{bmatrix}$, z_1 can be obtained from Eq. (19):

$$z_1(k) = E(y(k) - \tilde{C}_2 z_2(k) - \delta(k)) \tag{20}$$

where $E = K_1 R_1^{-1} G_s^T H_1^T$.

By replacing this expression of $z_1(k)$ in the second equation of (17) we obtain:

$$z_2(k+1) = \tilde{A}_{21} E[y(k) - \tilde{C}_2 z_2(k) - \delta(k)] + \tilde{A}_{22} z_2(k) + \tilde{B}_2 u(k) + \tilde{\omega}_2(k) \tag{21}$$

Finally we have the following dynamical system:

$$\begin{cases} z_2(k+1) & = A_2 z_2(k) + B_2 u(k) + D_2 y(k) - D_2 \delta(k) + \tilde{\omega}_2(k) \\ \tilde{y}_2(k) & = C_2 z_{2(k)} + H_{012}^T \delta(k) \end{cases} \tag{22}$$

where $A_2 = \tilde{A}_{22} - \tilde{A}_{21} E \tilde{C}_2$, $B_2 = \tilde{B}_2$, $C_2 = H_{012}^T \tilde{C}_2$ and $D_2 = \tilde{A}_{21} E$.

Assumption 2 *The pair (A_2, C_2) is detectable.*

To successfully design an interval observer for the discrete-time system in Eq. (22), the above assumption, which is standard in the field of observer design, is required [12]. Based on Assumption 2, the following lemma allows the transformation of system in Eq. (22) into a suitable form for interval observer design [13].

Lemma 1 *There exists a gain $L \in \mathbb{R}^{(n-q)\times(p-q)}$ and a transformation matrix P of appropriate dimensions such that $(A_2 - LC_2)$ is Schur stable and $R = P(A_2 - LC_2)P^{-1}$ is nonnegative.*

Such a transformation always exists, and in the case where the eigenvalues of $(A_2 - LC_2)$ are real, R can be chosen as diagonal or as Jordan form of $A_2 - LC_2$ [13]. After the change of coordinates $r_2 = Pz_2$, the system in Eq. (22) is described in the new coordinates by:

$$\begin{cases} r_2(k+1) & = Rr_2(k) + PB_2u(k) + My(k) - M\delta(k) + P\tilde{\omega}_2(k) \\ \tilde{y}_2(k) & = C_2P^{-1}r_{2(k)} + H_{012}^T\delta(k) \end{cases} \tag{23}$$

where $M = P(D_2 + LH_{012}^T)$.

B. Design of the interval observer

In this section, an interval observer is first designed for state estimation and then for unknown input estimation.

1. State estimation

The state estimation is first performed in the coordinates r_2. In the sequel, we define $\overline{\Delta}^T = \begin{bmatrix} \overline{\delta} & -\overline{\delta} \end{bmatrix}$, $\underline{\Delta}^T = \begin{bmatrix} -\overline{\delta} & \overline{\delta} \end{bmatrix}$ and $\overline{\Omega}^T = \begin{bmatrix} \overline{\omega} & -\overline{\omega} \end{bmatrix}$, $\underline{\Omega}^T = \begin{bmatrix} -\overline{\omega} & \overline{\omega} \end{bmatrix}$.

The following theorem allows us to carry out an interval state estimation in the coordinates r_2.

Theorem 1 *Assume that $\underline{r}_2(0) \leq r_2(0) \leq \overline{r}_2(0)$. Then, for all $k \in \mathbb{Z}_+$ the estimates $\underline{r}_2(k)$ and $\overline{r}_2(k)$ given by*

$$\begin{cases} \overline{r}_2(k+1) & = R\overline{r}_2(k) + PB_2u(k) + My(k) + (-M)^*\overline{\Delta} + P^*\overline{\tilde{\Omega}}_2 \\ \underline{r}_2(k+1) & = R\underline{r}_2(k) + PB_2u(k) + My(k) + (-M)^*\underline{\Delta} + P^*\underline{\tilde{\Omega}}_2 \end{cases} \tag{24}$$

are bounded and verify

$$\underline{r}_2(k) \leq r_2(k) \leq \overline{r}_2(k) \tag{25}$$

In addition, if the gain L is chosen such that $(A_2 - LC_2)$ is Schur stable, then $\overline{r}_2$ and $\underline{r}_2$ are bounded.

Furthermore, since $r_2 = Pz_2$, the bounds of $z_2(k)$ are given by the following corollary.

Corollary 1 *Under the conditions of Theorem 1, we have $\underline{z}_2(k) \leq z_2(k) \leq \overline{z}_2(k)$ with*

$$\begin{cases} \overline{z}_2(k) = (P^{-1})^+\overline{r}_2(k) + (P^{-1})^-\underline{r}_2(k) \\ \underline{z}_2(k) = (P^{-1})^+\underline{r}_2(k) + (P^{-1})^-\overline{r}_2(k) \end{cases} \tag{26}$$

The last step consists of computing the bounds for the entire state in the original coordinates $\underline{x}^T = \begin{bmatrix} \underline{x}_1 & \underline{x}_2 \end{bmatrix}$ and $\overline{x}^T = \begin{bmatrix} \overline{x}_1 & \overline{x}_2 \end{bmatrix}$. Based on Theorem 1 and Corollary 1, the following theorem ensures the interval estimation of the state x.

Theorem 2 *Assume that the conditions of Theorem 1 are satisfied and $\underline{x}(0) \leq x(0) \leq \overline{x}(0)$. Then, for all $k \in \mathbb{Z}_+$ the estimates $\underline{x}(k)$ and $\overline{x}(k)$ given by*

$$\begin{cases} \overline{x}_1(k) & = H_{11}Ey + (H_{12})^*\overline{Z}_2(k) + (-E_1)^*\overline{Z}_2(k) + (-H_{11}E)^*\overline{\Delta} \\ \underline{x}_1(k) & = H_{11}Ey + (H_{12})^*\underline{Z}_2(k) + (-E_1)^*\underline{Z}_2(k) + (-H_{11}E)^*\underline{\Delta} \\ \overline{x}_2(k) & = H_{21}Ey + (H_{22})^*\overline{Z}_2(k) + (-E_2)^*\overline{Z}_2(k) + (-H_{21}E)^*\overline{\Delta} \\ \underline{x}_2(k) & = H_{21}Ey + (H_{22})^*\underline{Z}_2(k) + (-E_2)^*\underline{Z}_2(k) + (-H_{21}E)^*\underline{\Delta} \end{cases} \tag{27}$$

are bounded and verify

$$\underline{x}(k) \leq x(k) \leq \overline{x}(k) \tag{28}$$

with $E_1 = H_{11}E\tilde{C}_2$ and $E_2 = H_{21}E\tilde{C}_2$.

2. Unknown input estimation

In this subsection, the upper and lower bounds of the unknown input d will be estimated. The expression of d is obtained from the first equation in Eq. (17):

$$d(k) = KR_0^{-1}[z_1(k+1) - \tilde{A}_{11}z_1(k) - \tilde{A}_{12}z_2(k) - \tilde{B}_1u(k) - \tilde{\omega}_1(k)] \tag{29}$$

By replacing z_1 with its expression in Eq. (20), Eq. (29) becomes:

$$d(k) = KR_0^{-1}[Ey(k+1) - E\tilde{C}_2z_2(k+1) - E\delta(k+1) - \tilde{A}_{11}(Ey(k) - E\tilde{C}_2z_2(k) - E\delta(k)) - \tilde{A}_{12}z_2(k) - \tilde{B}_1u(k) - \tilde{\omega}_1(k)] \tag{30}$$

The following theorem ensures the interval estimation of the unknown input d.

Theorem 3 *Assume that the conditions of Theorem 1 are satisfied. Then, for all $k \in \mathbb{Z}_+$ the estimates $\underline{d}(k)$ and $\overline{d}(k)$ given by*

$$\begin{cases} \overline{d}(k) & = Qy(k+1) - Q\tilde{A}_{11}Ey(k) - Q\tilde{B}_1u(k) + G_1^*\overline{Z}_2(k+1) + G_2^*\overline{Z}_2(k) + G_3^*\overline{\Delta} + G_4^*\overline{\Delta} + G_5^*\overline{\tilde{\Omega}}_1 \\ \underline{d}(k) & = QEy(k+1) - Q\tilde{A}_{11}Ey(k) - Q\tilde{B}_1u(k) + G_1^*\underline{Z}_2(k+1) + G_2^*\underline{Z}_2(k) + G_3^*\underline{\Delta} + G_4^*\underline{\Delta} + G_5^*\underline{\tilde{\Omega}}_1 \end{cases} \tag{31}$$

are bounded and verify

$$\underline{d}(k) \leq d(k) \leq \overline{d}(k) \tag{32}$$

With $Q = KR_0^{-1}$, $G_1 = -QE\tilde{C}_2$, $G_2 = Q(\tilde{A}_{11}E\tilde{C}_2 - \tilde{A}_{12})$, $G_3 = -QE$, $G_4 = Q\tilde{A}_{11}E$ and $G_5 = -Q$.

IV. Interval UIO for PMSM Speed and Unknown Load Torque Disturbance Estimation

In this section, the interval UIO presented in Section III.A is used to estimate the interval that contains the uncertainty on the PMSM speed and load torque. For this purpose, the linearized PMSM model in Eq. 13 is considered, and only the current measurements are assumed to be available. Moreover, modeling and measurement uncertainties are taken into account in the form of additive process and measurement noises that are respectively denoted as ω and δ. Finally, the discrete-time form of the continuous-time model is used for the interval UIO implementation.

A. Simulation parameters

The parameters of the PMSM under consideration were taken from Ref. [14] and are listed in Table 1. All simulations were conducted using a MATLAB simulation environment. The model and measurement noises are assumed to be uniformly distributed and bounded by

$\overline{\omega} = 10^{-2}\begin{bmatrix}1 & 1 & 1\end{bmatrix}^\top$ and $\overline{\delta} = 10^{-2}\begin{bmatrix}1 & 1 & 1\end{bmatrix}^\top$.

Finally, the bounds of the initial state vector are chosen as

$\underline{x_0} = 10^{-2}\begin{bmatrix}1 & 1 & 1\end{bmatrix}^\top$ and $\overline{x_0} = 10^{-2}\begin{bmatrix}1 & 1 & 1\end{bmatrix}^\top$.

The motor speed and unknown load torque bounds were computed under different scenarios to demonstrate the impact of operating conditions on the estimations:

1) Step load torque from 0 to 2 Nm is applied at 0.25 sec.
2) Initial constant load torque of 2 Nm, then sinusoidal disturbance is applied at 0.25 sec.
3) Ramp speed variation

Table 1 PMSM parameters

Parameter	Symbol	Value
Number of pole pairs	n_p	1
Stator resistance	R_s	1.4 Ω
Stator inductance	L_s	0.73 mH
Stator mutual inductance	M_s	73 μH
Permanent magnet flux	λ_M	0.1546 Wb
Rotor inertia	J	$60 \cdot 10^{-6}$ kgm^2

B. Results and Discussion

In this section, we present and discuss the results of the interval estimations of the motor speed and unknown load torque under the three different scenarios described in Section IV.A.

The results obtained for the first scenario (step load torque from 0 to 2 Nm at 0.25 sec) are shown in Fig. 1 for the load torque and in Fig. 2 for the speed. The upper and lower bounds of the load torque are well estimated and they always bound the reference unknown load torque despite the step perturbation applied at 0.25 sec. As for the speed interval estimation in Fig. 2, the estimated bounds are very close to the reference speed but do not always bound it. However, it is shown in Fig. 3 that even when a perturbation in the load torque is applied, the interval UIO is still able to estimate the corresponding perturbation in the speed.

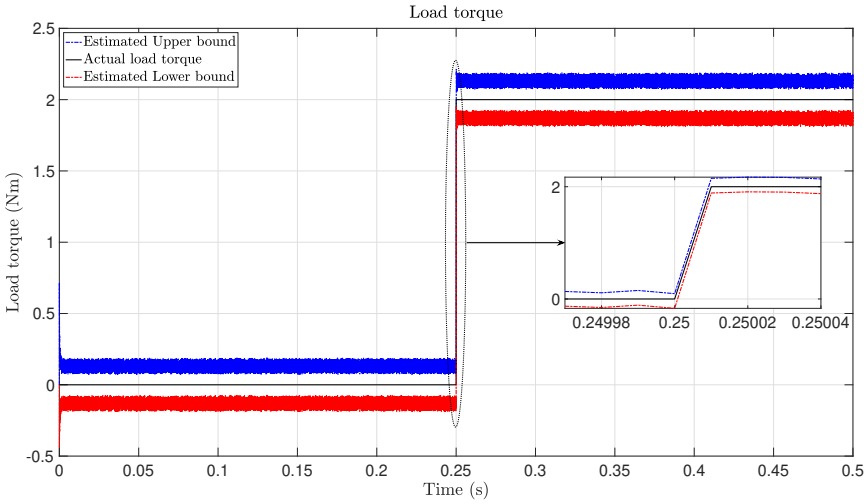

Fig. 1 Step load torque estimation

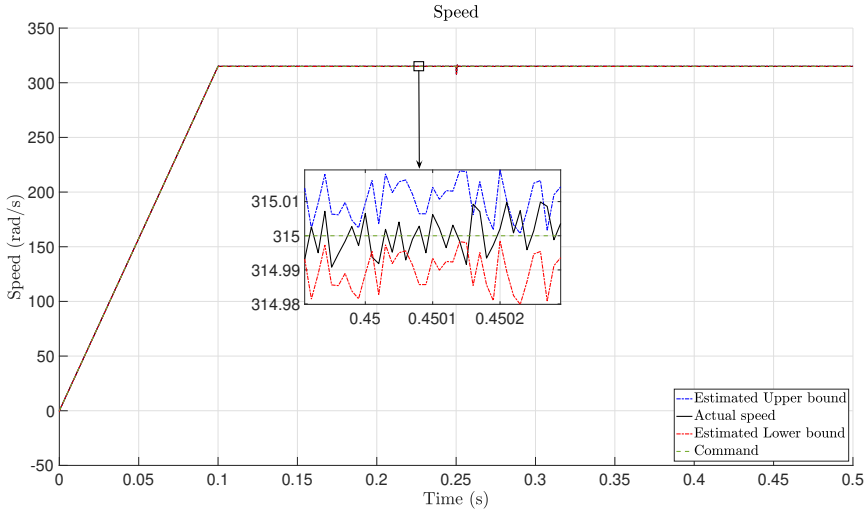

Fig. 2 Speed estimation with step load torque

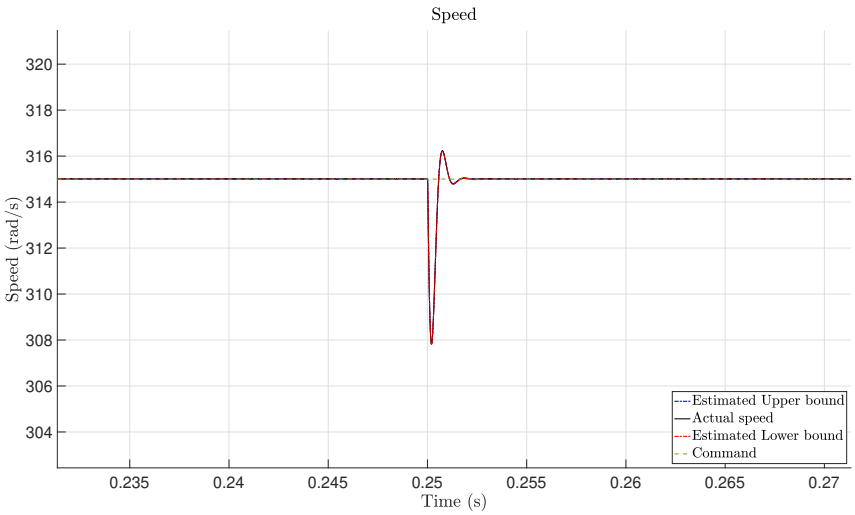

Fig. 3 Speed estimation: Centered at step load torque application

In Fig. 4 and Fig. 5, we present the estimation results of the load torque and speed bounds, respectively, for the second scenario in which a constant then sinusoidal load torque is applied. Fig. 4 shows that the interval UIO is successfully able to estimate the constant and subsequently sinusoidal shape of the unknown load torque.The estimated bounds of the speed are very close to the reference speed (Fig. 5), even after the sinusoidal disturbance was applied (Fig. 6).

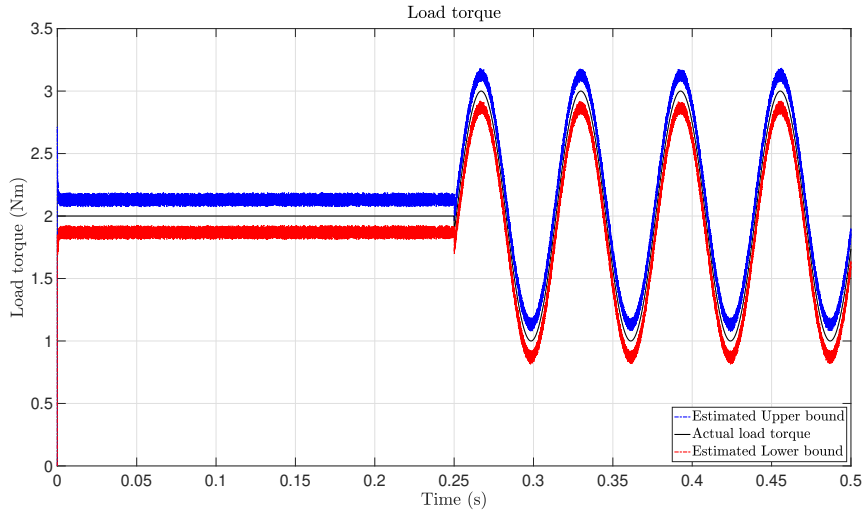

Fig. 4 Sinusoidal load torque estimation

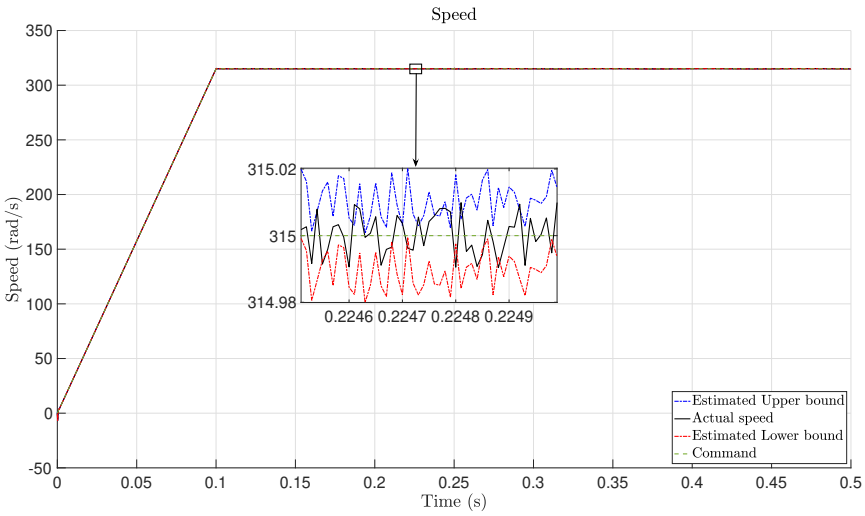

Fig. 5 Speed estimation for sinusoidal load torque

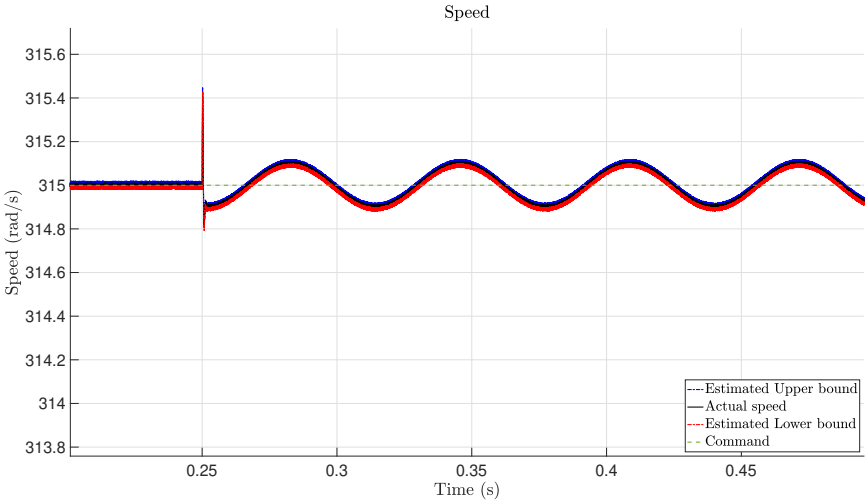

Fig. 6 Speed estimation (zoomed in) for sinusoidal load torque

Finally, Fig. 7 depicts the simulation results for the third scenario in which the motor speed is changed. The motor speed is initially accelerated according to a ramp shape, and after running at a constant speed until 0.35 sec, the motor velocity is decreased. Fig. 7 demonstrates that the interval UIO successfully estimates and reproduces the variations of the speed.

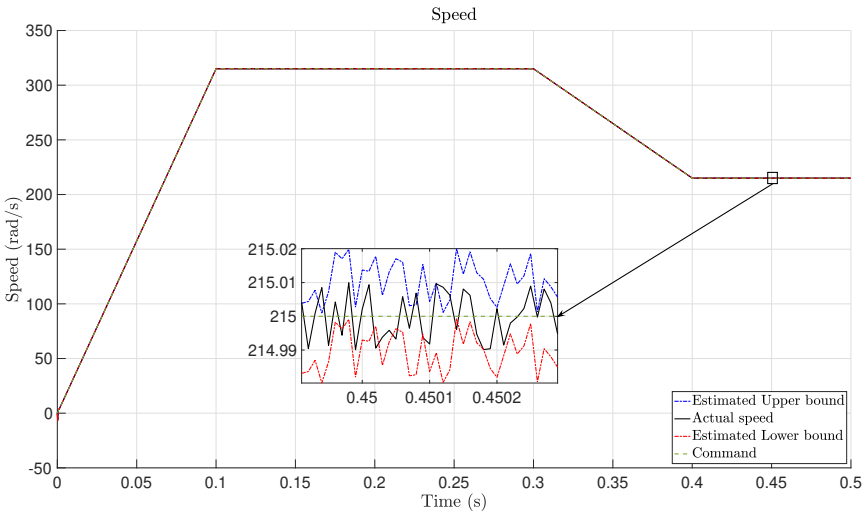

Fig. 7 Variable speed

In the three different scenarios, the interval UIO managed to reconstruct the bounds of both the changing speed and load torque for the PMSM. Their variations were also well captured by the observer. However, for the reference speed, although very close to the reference, the estimated upper and lower bounds did not always contain/bound the speeds and contained slight errors, less than one percent. The nonlinear PMSM model utilized was linearized using a first order Taylor series expansion, possibly inducing model errors that affect the estimation process with the linear interval UIO. To circumvent this error in estimating the speed bounds, a non linear interval UIO could be synthesized. However, the system has to be transformed into a canonical form, which may be difficult in practice. For this reason, we may choose to represent the system by a Linear Parameter Varying (LPV) model. Using the LPV form will reduce the linearization errors while allowing the use of tools developed in the context of linear systems.

V. Conclusion

In this paper, an interval unknown input observer (UIO) has been utilized to jointly estimate the speed and unknown load torque of a permanent magnet synchronous motor (PMSM). The estimation of these two variables is required for fault detection and failure prediction of PMSM components that will enable safety of emerging operations, such as Urban Air Mobility (UAM). Employing an interval UIO allows the joint estimation of both the speed and unknown load torque while accounting for uncertainties related to model and measurements errors. The simulation results showed that the linear interval UIO accurately estimates the upper and lower bounds of the unknown load torque but does not estimate the speed bounds as accurately. Due to errors inherently associated with linearization and loss of the nonlinear system characteristics, the interval estimation is not always guaranteed. Thus, further work should be done to develop a Linear Parameter Varying form of the PMSM model to reduce the model errors. This will enable future utilization of the various estimation frameworks developed for linear systems.

Acknowledgments

This work was supported by the System-Wide Safety (SWS) project under the Airspace Operations and Safety Program within the NASA Aeronautics Research Mission Directorate (ARMD).

References

[1] Ellis, K., Krois, P., Davies, M. D., and Koelling, J., "In-Time System-Wide Safety Assurance (ISSA) Concept of Operations," 2019.

[2] Ellis, K. K., Krois, P., Koelling, J., Prinzel, L. J., Davies, M., and Mah, R., "A Concept of Operations (ConOps) of an In-time Aviation Safety Management System (IASMS) for Advanced Air Mobility (AAM)," *AIAA Scitech 2021 Forum*, 2021, p. 1978.

[3] Sirimanna, S., Thanatheepan, B., Lee, D., Agrawal, S., Yu, Y., Wang, Y., Anderson, A., Banerjee, A., and Haran, K., "Comparison of Electrified Aircraft Propulsion Drive Systems with Different Electric Motor Topologies," *Journal of Propulsion and Power*, 2021, pp. 1–15.

[4] Colucci, B. F., "Turning Volts to VTOL," 2016, pp. 30–33.

[5] Henke, M., Narjes, G., Hoffmann, J. M., Wohlers, C., Urbanek, S., Heister, C., Steinbrink, J., Canders, W.-R., and Ponick, B., "Challenges and Opportunities of Very Light High-Performance Electric Drives for Aviation," 2018.

[6] Bowen, C., Jihua, Z., and Zhang, R., "Modeling and simulation of permanent magnet synchronous motor drives," *ICEMS'2001. Proceedings of the Fifth International Conference on Electrical Machines and Systems (IEEE Cat. No. 01EX501)*, Vol. 2, IEEE, 2001, pp. 905–908.

[7] Park, R. H., "Two-reaction theory of synchronous machines generalized method of analysis-part I," *Transactions of the American Institute of Electrical Engineers*, Vol. 48, No. 3, 1929, pp. 716–727.

[8] Vyncke, T., Boel, R., and Melkebeek, J., "A comparison of stator flux linkage estimators for a direct torque controlled PMSM drive," *35th Annual Conference of IEEE Industrial Electronics*, 2009, pp. 971–978.

[9] Robinson, E. I., Marzat, J., and Raïssi, T., "Interval observer design for unknown input estimation of linear time-invariant discrete-time systems," *IFAC-PapersOnLine*, Vol. 50, No. 1, 2017, pp. 4021–4026.

[10] Robinson, E., Marzat, J., and Raïssi, T., "Prognosis of uncertain linear time-invariant discrete systems using unknown input interval observer," *International Journal of Control*, 2019, pp. 1–17.

[11] Maquin, D., Gaddouna, B., and Ragot, J., "Estimation of unknown inputs in linear systems," *Proceedings of American Control Conference, Baltimore, MD*, Vol. 1, 1994, pp. 1195–1197.

[12] Hou, M. and Muller, P., "Design of observers for linear systems with unknown inputs," *IEEE Transactions on Automatic Control*, Vol. 37, No. 6, 1992, pp. 871–875.

[13] Efimov, D., Perruquetti, W., Raïssi, T., and Zolghadri, A., "On interval observer design for time-invariant discrete-time systems," *European Control Conference (ECC), Zurich, Swiss*, 2013, pp. 2651–2656.

[14] Otava, L. and Buchta, L., "Implementation and verification of the PMSM stator interturn short fault detection algorithm," *19th European Conference on Power Electronics and Applications (EPE'17 ECCE Europe)*, IEEE, 2017, pp. 1–10.